Biotechnology and Bioprocess Engineering 23: 532-540 (2018)
DOI 10.1007/s12257-018-0190-z

pISSN 1226-8372
eISSN 1976-3816

RESEARCH PAPER

Kinetics and Mechanism of Ultrasound-assisted Extraction of Paclitaxel from *Taxus chinensis*

Kyung-Wan Yoo and Jin-Hyun Kim

Received: 28 May 2018 / Revised: 16 July 2018 / Accepted: 21 July 2018

Abstract Batch experimental studies were carried out for the ultrasound-assisted extraction of paclitaxel from *Taxus chinensis* while varying parameters such as ultrasound power, extraction temperature and contact time. The extraction of the majority of the paclitaxel (~99%) was achieved from the biomass by a single extraction at 380 W of ultrasound power for a period of 10 min. The kinetics data obtained for the paclitaxel extractions, and the dominant role played by intraparticle diffusion, were found to be in concordance with the pseudo-second-order model, and the intraparticle diffusion model respectively. The effective diffusion coefficient of paclitaxel ($4.1882 \times 10^{-13} \sim 5.7093 \times 10^{-13}$ m^2/s) and the mass transfer coefficient ($4.705 \times 10^{-8} \sim 14.1160 \times 10^{-8}$ m/s) increased when the extraction temperature and ultrasound power were raised.

Keywords: paclitaxel, ultrasound-assisted extraction, kinetics, effective diffusion coefficient, mass transfer coefficient

1. Introduction

Paclitaxel, a complex diterpenoid alkaloid, was originally isolated from the bark extract of the pacific yew tree, *Taxus brevifolia*. It has been one of the most successful and effective antitumor agents of recent decades, and is used to treat ovarian, breast, lung, Kaposi's sarcoma, head and neck cancers [1,2]. In addition, its efficacy in the treatment of rheumatoid arthritis and Alzheimer's disease is currently being explored, with clinical trials being conducted on various combinations of therapies, leading to the likely steady increase in demand for paclitaxel in the future [3,4]. The most widely utilized methods for the production of paclitaxel include direct extraction from the bark of the yew tree [5], semi-synthesis involving the chemical bonding of side chains to precursors such as baccatin III, 13-dehydroxybaccatin III, 10-deacetylbaccatin III and 10-deacetylpaclitaxel obtained from the leaves of the yew tree [6], and plant cell culturing by the induction of callus from yew explants [7]. The direct extraction method leads to the destruction of scarce plant material combined with a difficulty in consistently suppling the raw materials. Meanwhile, semi-synthesis of paclitaxel is very complex and results in a very low yield. By contrast, plant cell culturing enables the stable mass production of paclitaxel, of a consistent quality, in a bioreactor without any interference from environmental factors [1].

In plant cell cultures, paclitaxel produced through metabolic pathways is mostly accumulated in plant cells (biomass) [8]. It is essential to first recover the paclitaxel from the biomass for its efficient isolation and purification. In general, a conventional solvent extraction is the most widely used means for the recovery of paclitaxel from biomass. The effects of extraction conditions on the conventional solvent extraction method's efficiency has been investigated, and the extraction conditions have been optimized [1,9]. However, this conventional method requires a long extraction time with large amounts of organic solvent and results in a low extraction efficiency. Even under optimum extraction conditions, at least four extractions are needed to recover the majority of the paclitaxel (~99%). Recently, ultrasound-assisted extraction has been widely touted as an effective, environmentally friendly, safe, reliable and inexpensive technology, able to increase the efficiency in the extraction of a variety of bioactive substances from biomass [10-14].

Kyung-Wan Yoo, Jin-Hyun Kim*
Department of Chemical Engineering, Kongju National University, Cheonan 330-717, Korea
Tel: +82-41-521-9361; Fax: +82-41-554-2640
E-mail: jinhyun@kongju.ac.kr

Ultrasound-assisted extraction is based on the principle of acoustic cavitation, which is capable of damaging the cell walls of the plant matrix, thereby favoring the release of bioactive compounds from the matrix into the solvent. However, most previous studies have focused on optimizing the experimental conditions or process parameters and a qualitative description of their effects, with very little quantitative analysis of the mechanism and kinetics of ultrasound-assisted extraction [10-14]. Kinetic data provides information about the pathway, rate, and extent of the reaction [15,16]. In particular, the kinetic model is a useful engineering tool, considerably facilitating design, optimization, and simulation of the extraction process, and contributing to better utilization of energy, solvents, and time. Therefore, this study has systematically investigated the effects of ultrasound power, temperature, and time on the extraction yields of paclitaxel from biomass, and then analyzed the kinetics of the ultrasound-assisted extraction process. In addition, the effective diffusion coefficient, mass transfer coefficient and Biot number were determined under various extraction conditions, so as to understand the mechanism of mass transfer in the extraction.

2. Materials and Methods

2.1. Plant materials

Suspension cells originating from *Taxus chinensis* were cultured in a dark bioreactor at 24°C [7]. After culturing, the plant cells were recovered from the culture broth using a decanter (CA150 Clarifying Decanter; Westfalia) and a high-speed centrifuge (BTPX 205GD-35CDEFP; Alfa-Laval). The plant cells (biomass) for this study were provided by the Samyang Biopharm Company, South Korea.

2.2. Paclitaxel analysis

The paclitaxel content was analyzed using an HPLC system (SCL-10AVP, Shimadzu, Japan) equipped with a Capcell Pak C18 column (250 mm × 4.6 mm; Shiseido). The mobile phase involved the mixture of acetonitrile and distilled water (35:65 ~ 65:35, v/v, gradient mode) at a flow rate of 1.0 mL/min. The effluent was monitored at 227 nm with a UV detector with the injection volume being 20 mL [15]. Authentic paclitaxel (purity: 95%) was used as the standard. Each sample was analyzed in triplicate.

2.3. Ultrasonic bubble observation

The distribution of bubbles was observed during ultrasound-assisted extraction using an EOS 650D digital camera (Canon, Japan) with an EF-S 18-55 mm lens. The image size obtained from the digital camera was set to 2,481 × 1,654. The shutter speed was set to 1/2,500 sec, and the ISO sensitivity was set at 3,200.

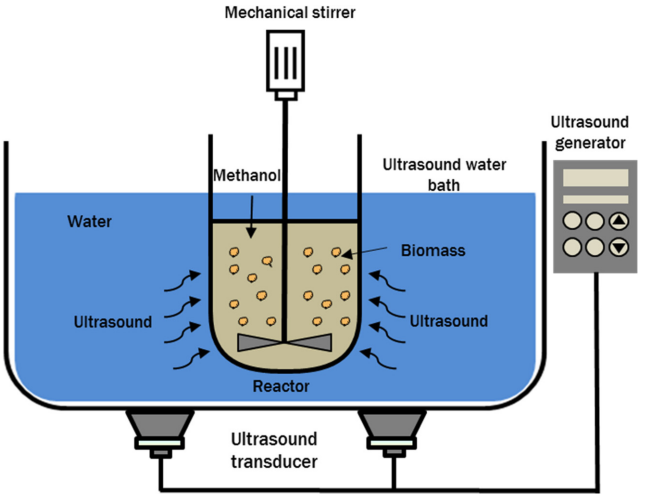

Fig. 1. Schematic diagram of the ultrasound-assisted extraction process.

2.4. SEM analysis

The surface structure and morphology of the biomass before and after extraction were observed using a scanning electron microscope (MIRA LMH; Tescan, Czech Republic) at an electron acceleration voltage of 10-15 kV. The sample used in the analysis was about 1 mg.

2.5. Ultrasound-assisted extraction

The ultrasound-assisted extraction was carried out with a 1:1 (w/v) ratio of biomass to methanol and two 40 kHz ultrasonic cleaners, one with a maximum power output of 250 W (UC-10, Jeiotech, South Korea) and the other of 530 W (JAC-4020, KODO, South Korea) [17]. The biomass was extracted at different temperatures (298, 303, 308, 313, and 318 K), ultrasound powers (80, 180, 250, 380, and 530 W), and operational times (1, 2, 4, 6, 8, 10, 12, 15, and 30 min) with a stirring speed of 500 rpm. The extraction temperature was selected considering the degradation of paclitaxel at high temperature (>323 K) [17]. Fig. 1 shows a schematic diagram of the ultrasound-assisted extraction process. The reactor (Pyrex glass beaker) containing the sample was placed in an ultrasonic water bath and the experiment was carried out. The reactor size and working volume were 100 and 30 mL, respectively. After the extraction, the mixture was filtered in a vacuum using filtration paper (150 mm, Whatman). The filtrate (methanol extract) was collected, concentrated using a concentrator (CCA-1100, EYELA, Japan), and then completely dried in a vacuum (40°C, overnight). The purity of the crude extract was

measured using HPLC. The paclitaxel yield (Y, %) was calculated using Eq. (1):

$$Y\ (\%) = \frac{Q_E}{Q_B} \times 100 \quad (1)$$

where Q_E is the quantity of paclitaxel in the crude extract and Q_B is the quantity of paclitaxel in the biomass. All the experiments were performed in triplicate and the average values from the results were taken.

2.6. Kinetic models

In an extraction study, it is necessary to apply the extraction data to different models and equations in order to analyze the kinetics of the extraction process. The pseudo-first-order model [18], pseudo-second-order model [19,20], and intraparticle diffusion model [21] were used for kinetic analysis. The effective diffusion coefficient and mass transfer coefficient were calculated by applying Fick's law [22-24]. The relative magnitudes of external and internal resistances to mass transfer were determined using Biot number (Bi) [22]. Table 1 summarizes the equations used for parameter estimation. The validity of the models was evaluated by the coefficient of determination (r^2) and the root mean squared deviation (RMSD) [17]. The RMSD can be expressed as Eq. (2):

$$RMSD = \sqrt{\frac{1}{n}\sum_{i=1}^{n}(experimental - calculated)^2} \quad (2)$$

where n is the number of experimental runs.

3. Results and Discussion

3.1. Influence of ultrasound power and extraction temperature

In order to investigate the effects of ultrasound power on the efficiency of ultrasound-assisted extraction, the extraction was performed using different ultrasound powers (80, 180, 250, 380, and 530 W) and extraction times (1, 2, 4, 6, 8, 10, 12, 15, and 30 min) at a fixed biomass/methanol ratio (1:1, w/v), temperature (298 K), stirring speed (500 rpm), and extraction number (1). As shown in Fig. 2, the yield of paclitaxel increased with increasing ultrasound power and time, while the highest yield (~99%) was obtained when ultrasound power at 380 W was applied over a period of 10 min. It was observed that when the ultrasound power was below 380 W, the paclitaxel yield (~80%) did not significantly increase after 10 min of extraction time. These results indicate that cell destruction is more widespread

Table 1. Equations used for parameter estimation

Equation	Parameter	Ref.
$\ln(C_e - C_t) = \ln C_e - k_1 t$	C_t (mg/mL): concentration of paclitaxel in the suspension at any time C_e (mg/mL): concentration of extracted paclitaxel at equilibrium k_1 (min^{-1}): pseudo-first-order rate constant	[18]
$\frac{t}{C_t} = \frac{1}{k_2 C_e^2} + \frac{t}{C_e}$ $h = k_2 C_e^2$	k_2 (mL/mg·min): pseudo-second-order rate constant h (mg/mL·min): initial extraction rate	[19,20]
$q_t = k_p t^{1/2}$	q_t: yield of paclitaxel extracted in the suspension at time t k_P ($mg/g \cdot min^{1/2}$): intraparticle diffusion rate constant	[21]
$\ln\left(\frac{Y_s}{Y_s - Y_t}\right) = \ln\frac{\pi^2}{6} + \frac{D_e \pi^2 t}{R^2}$	Y_s: total paclitaxel yield at saturation Y_t: total paclitaxel yield at time t D_e (m^2/s): effective diffusion coefficient R: cell radius (average radius: 42.5×10^{-6} m)	[22]
$\ln\frac{C_s}{C_s - C_t} = \frac{K_T A}{V_s} t$ $A = \frac{3 m_{plant}}{\rho r_p}$	C_s (mg/mL):saturation concentration of paclitaxel C_t (mg/mL): concentration of paclitaxel at time t A (m^2): total surface area of the particles (cells) m_{plant} (kg):cell weight introduced in the extractor ρ: cell wet density (1071.43 kg/m^3) r_p: cell size (average radius: 42.5×10^{-6} m) V_s (m^3): volume of solution K_T (m/s): mass transfer coefficient	[23,24]
$Bi = \frac{r_p K_T}{D_e}$	Bi: Biot number	[24]

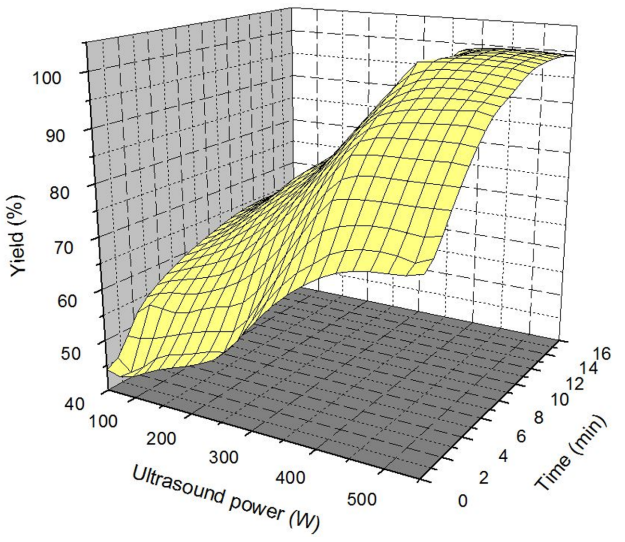

Fig. 2. 3D response surface and contour plots for the optimization of the ultrasound-assisted extraction process from *Taxus chinensis*. The biomass/MeOH ratio, temperature, and stirring speed were 1:1 (w/v), 298 K, and 500 rpm, respectively.

when the ultrasound power is increased, resulting in an improved extraction efficiency [25]. Hence, a single extraction under optimum ultrasound power (380 W) and duration (10 min) recovered the majority of paclitaxel (~99%) from the biomass. On the other hand, in the absence of ultrasound, most of the paclitaxel (~99%) was recovered by extraction at least four times [1, 9].

The propagation of ultrasonic waves in liquid medium can generate cavitation bubbles due to the pressure variation [26]. The trends in cavitation bubble formation according to ultrasound power (80, 180, 250, and 380 W) were investigated using a digital camera (Fig. 3). The number of cavitation bubbles was seen to increase with greater ultrasound power. This is because the number of cavitation bubbles generated at a certain ultrasonic frequency depends on the ultrasound power [26]. The collapse of these bubbles can locally result in extremely high pressure and temperature, thus facilitating the destruction of surface material. For this reason, the extraction efficiency increases as the ultrasound power increases.

The surface structure and shape of the biomass were investigated through SEM analysis. In the case of the biomass before extraction (Fig. 4A), the surface was relatively smooth and nonporous. After conventional solvent extraction (Fig. 4B), the biomass became atrophic with the appearance of ruptures and wrinkles. Meanwhile, after ultrasound-assisted extraction (Figs. 4C-4E), the biomass appeared completely disrupted, with all the cell walls being broken or damaged and significant changes in the cell shapes as ultrasound power increased. This result was probably related to the shear forces of ultrasonic cavitation. Therefore, the disruption of the biomass surface, which favored the mass transfer of paclitaxel into the solution, resulted in a dramatically improved extraction efficiency. These results are reasonable since the increase of ultrasonic energy dissipated in the extractor can improve the mechanical and cavitation effects of ultrasound. Similar results were obtained in the study of ultrasound-assisted extraction of bioactive substance from *Achillea biebersteinii*, in which it was also found that an increase in the output of ultrasonic energy promoted biomass disruption [25].

The effects of the extraction temperature on the extraction

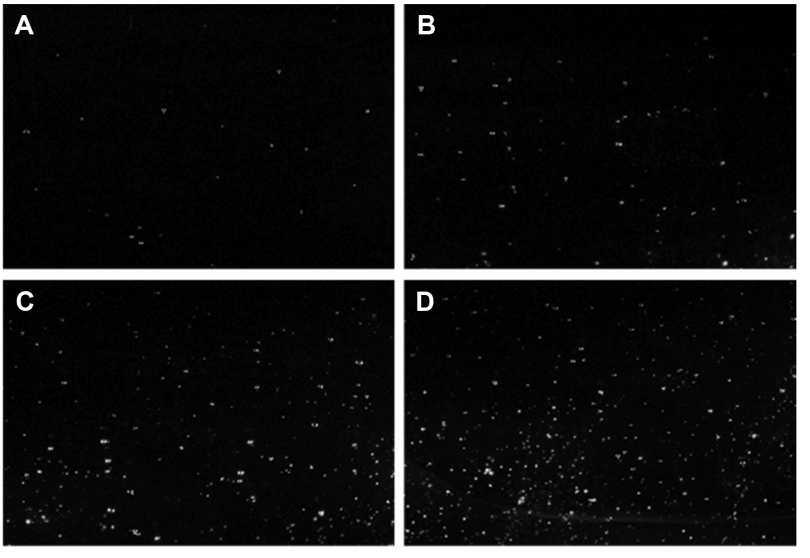

Fig. 3. Bubble cloud images at ultrasound power 80 W (A), ultrasound power 180 W (B), ultrasound power 250 W (C), and ultrasound power 380 W (D).

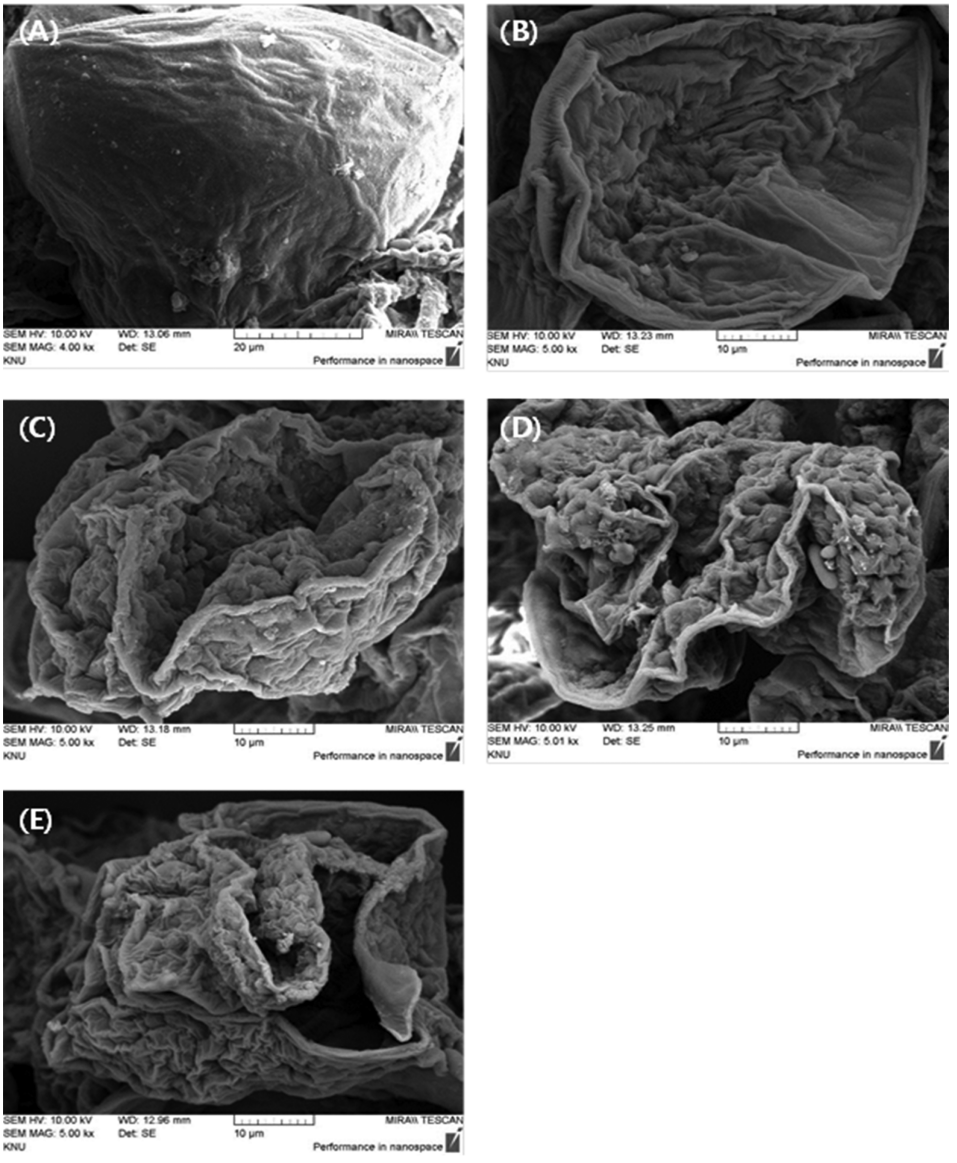

Fig. 4. SEM images of untreated (A), conventional solvent extraction-treated (B), ultrasound-assisted extraction (ultrasound power 180 W)-treated (C), ultrasound-assisted extraction (ultrasound power 250 W)-treated (D), ultrasound-assisted extraction (ultrasound power 380 W)-treated, and (E) biomasses.

efficiency of paclitaxel from the biomass were investigated. When using temperatures (298, 303, 308, 313, and 318 K), the ultrasound-assisted extraction was performed once using various ultrasound powers (180, 250, and 380 W) and extraction times (1, 2,4, 6, 8, 10, 12, 15, and 30 min). When using an ultrasound power between 180 and 250 W (Fig. 5A and 5B), the yield of paclitaxel in all treatments increased markedly in the first 10 min of sonication and then increased slowly and steadily thereafter until reaching equilibrium. The maximum yield of paclitaxel was 75-82% and 80-87% at 180 W and 250 W, respectively. The maximum yields and initial extraction rates of the extracted paclitaxel all increased when more ultrasound power and higher extraction temperatures were applied. Meanwhile, when using an ultrasound power of 380 W (Fig. 5C), the yield of paclitaxel increased sharply until 10 min of extraction at 298 K and 303K, until 8 min of extraction at 303 K and 308 K, and until 6 min of extraction at 318 K, respectively. Thereafter, the yield of paclitaxel increased slowly and steadily until reaching equilibrium, and almost all of the paclitaxel was recovered (~99%) at the same time. This result indicates that a rise in ultrasound power and temperature increases the solubility and facilitates the diffusion of paclitaxel while reducing the viscosity of the extraction solution [17,27].

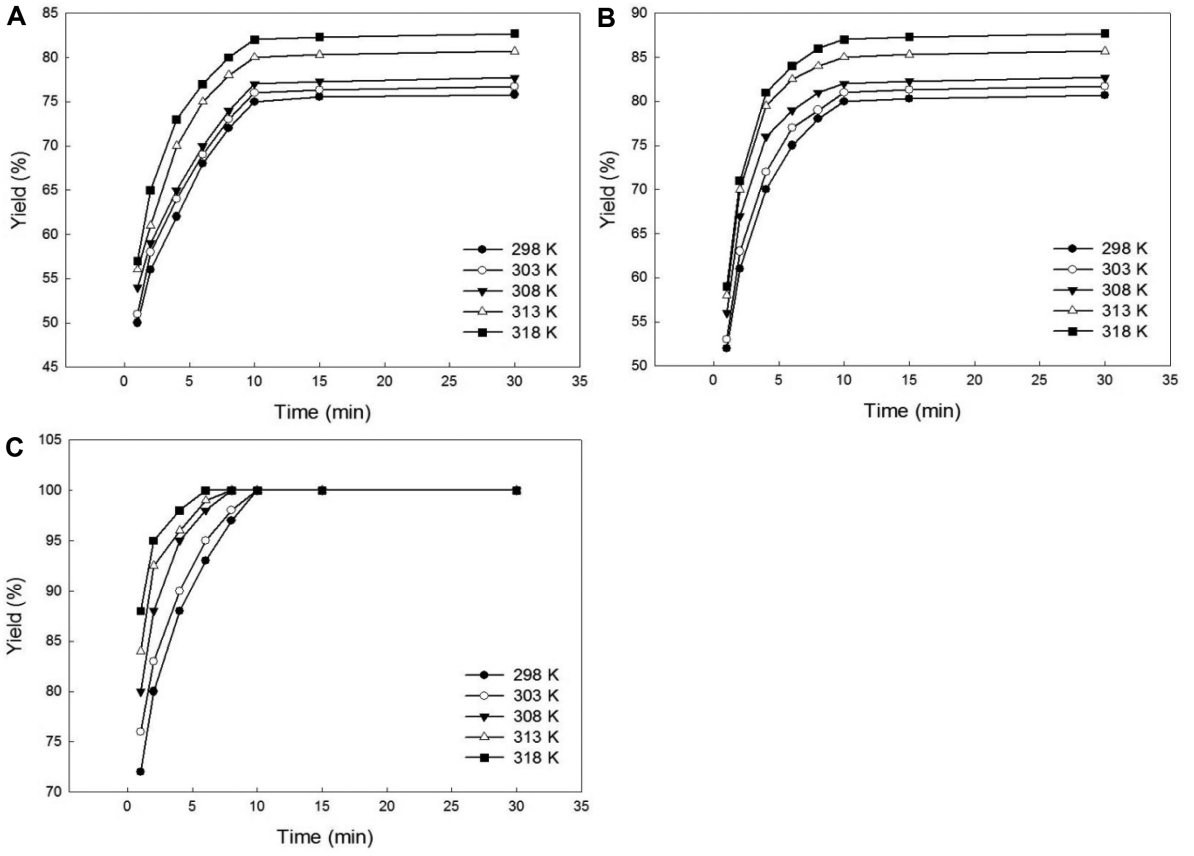

Fig. 5. Effect of temperature on the yield of paclitaxel during ultrasound-assisted extraction at different ultrasound powers. (A) ultrasound power 180 W; (B) ultrasound power 250 W; (C) ultrasound power 380 W. The biomass/MeOH ratio, stirring speed were 1:1 (w/v) and 500 rpm, respectively.

3.2. Kinetic analysis

Pseudo-first-order and pseudo-second-order kinetic models were used to analyze the experimental data for the ultrasound-assisted extraction of paclitaxel from biomass. The applicability of each model was identified using r^2 and RMSD, while the ultrasound-assisted extraction pattern was quantitatively investigated using a kinetic analysis.

As a result of the comparison of kinetic models, it was found that the pseudo-second-order model was more suitable for the extraction of paclitaxel from the biomass in terms of the r^2 and RMSD. For the pseudo-second-order model, t/C_t and t were plotted, and k_2 and C_e were calculated from the slope and the intercept. The parameters obtained from the kinetic equation together with the r^2 and RMSD, are listed in Table 2. The values of h and k_2 increased when increasing the temperature and ultrasound power, meaning the initial extraction rate and overall extraction rate were also increased. Similar solid-liquid extraction behaviors have also been reported in previous studies [13,19,20,28]. Compared to conventional solvent extraction [16], the extraction rate constants increased up to 2.2, 2.3, 2.8, 4.1, and 4.6 times at 298, 303, 308, 313, and 318 K, respectively. In particular, the extraction rate constant increased markedly at 380 W than at 180 W and 250 W of ultrasound power at all the investigated temperatures. Since the changes in h and k_2 were smaller than those previously reported for the extraction of bioactive substances from pomegranate peel [13], the extraction process in this study appeared relatively insensitive to ultrasound power. In addition, the value of C_e increased when increasing the temperature and ultrasound power. This improved extraction efficiency was attributed to an increased solubility and easier diffusion of the paclitaxel due to the increased temperature and ultrasound power [12,27]. Therefore, for the biomass recovery of paclitaxel using ultrasound-assisted extraction, the pseudo-second-order model was suitable, showing a large value for r^2 (>0.9965) and a small value for RMSD (<0.0098).

The intraparticle diffusion model proposed by Weber and Morris [21] was applied to determine if the rate-limiting step is intraparticle diffusion. According to Table 1, a plot of q_t versus $t^{1/2}$ should be in a straight line with a slope k_p when the extraction mechanism follows the intraparticle diffusion process [29]. As shown in Fig. 6, the plot was multi-linear and there were three different portions, indicating

Table 2. Parameters of pseudo-second-order model for the ultrasound-assisted extraction of paclitaxel from *Taxus chinensis*

Model	Ultrasound power (W)	Parameter	Temperature (K)				
			298	303	308	313	318
Second- order model	180	h (mg/mL·min)	0.2765	0.3004	0.3219	0.3581	0.4030
		k_2 (mL/mg·min)	4.8169	5.1502	5.4327	5.5322	5.9974
		C_e (mg/mL)	0.2399	0.2417	0.2436	0.2548	0.2592
		r^2	0.9995	0.9970	0.9965	0.9996	0.9998
		RMSD	0.0097	0.0077	0.0098	0.0066	0.0049
	250	h (mg/mL·min)	0.3302	0.3616	0.4726	0.5218	0.5512
		k_2 (mL/mg·min)	5.0159	5.3995	7.0243	7.2320	7.3069
		C_e (mg/mL)	0.2566	0.2589	0.2595	0.2687	0.2748
		r^2	0.9993	0.9996	0.9999	0.9997	0.9995
		RMSD	0.0056	0.0052	0.0077	0.0077	0.0049
	380	h (mg/mL·min)	0.6838	0.7969	1.0659	1.6428	2.0222
		k_2 (mL/mg·min)	7.7714	8.8499	11.7377	17.7250	21.7468
		C_e (mg/mL)	0.2966	0.3000	0.3014	0.3044	0.3049
		r^2	0.9985	0.9992	0.9999	0.9999	0.9999
		RMSD	0.0077	0.0067	0.0075	0.0065	0.0035

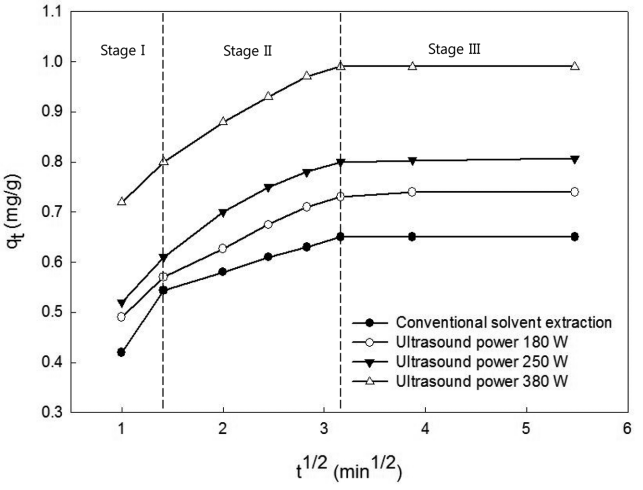

Fig. 6. Intraparticle diffusion plot for the ultrasound-assisted extraction of paclitaxel at 298 K.

three different stages in extraction. The first portion (Stage I) is the washing step with rapid solute transfer from the surface of the solid into the bulk of liquid, and the second portion (Stage II) is the diffusion step with slower, prolonged transfer of solutes from the solid interior to the solid surface. The third portion (Stage III) is the equilibrium step, where the extraction reaches near equilibrium, resulting in a slow diffusion. Generally, the third stage is very rapid and does not constitute a rate-limiting step in the extraction [29]. In conventional solvent extraction, the washing step and the diffusion step of the extraction are clearly distinguished, and extraction proceeds step by step. On the other hand, in ultrasound-assisted extraction, the washing step and the diffusion step of the extraction are not clearly distinguished due to the ultrasonic waves; therefore, the extraction of these latter two steps is almost simultaneous. This phenomenon was seen to be more pronounced as ultrasound power was increased. It was also found that the extraction of paclitaxel from the biomass followed the intraparticle diffusion model after 2 min. In addition, the linear line did not pass through the origin, which indicates that intraparticle diffusion is not the only rate limiting mechanism in the extraction process. Since the value of k_p in the washing step (Stage I) is greater than that of k_p in intraparticle diffusion (Stage II), the latter affected the rate-limiting step more significantly. Also, it was observed that the rate constant in the diffusion step increased in the following order: conventional solvent extraction (0.0612 mg/g·min$^{1/2}$) < ultrasound power 180 W (0.0939 mg/g·min$^{1/2}$) < ultrasound power 250 W (0.1086 mg/g·min$^{1/2}$) < ultrasound power 380 W (0.1102 mg/g·min$^{1/2}$). From the viewpoint of the extraction rate, it was found that ultrasound-assisted extraction was more effective than conventional solvent extraction and the extraction rate increased with increasing ultrasound power.

3.3. Estimation of effective diffusion coefficient and mass transfer coefficient

The diffusion model based on Fick's second law was used to describe the mass transfer of a solute from the spherical solid interior to the solid surface [22]. Meanwhile, the analytical expression of the diffusive flux, based on Fick's first law, was used to explain the mass transfer of a solute

Table 3. Values of the effective diffusion coefficient D_e, the mass transfer coefficient K_T, Biot number Bi obtained for the ultrasound-assisted extraction of paclitaxel from *Taxus chinensis*

Ultrasound power (W)	Temperature (K)	$D_e \times 10^{13}$ (m^2/s)	$K_T \times 10^8$ (m/s)	Bi
180 W	298	4.1882	4.7053	4.7747
	303	4.3362	5.0089	4.9093
	308	4.5042	5.4642	5.1559
	313	4.6107	6.0714	5.5964
	318	4.7882	6.8303	6.0626
250 W	298	4.3319	5.0089	4.9142
	303	4.5404	5.4642	5.1148
	308	4.7621	6.5267	5.8248
	313	5.0608	7.5892	6.3734
	318	5.3915	8.3482	6.5806
380 W	298	5.0598	7.7410	6.5021
	303	5.2202	8.6517	7.0437
	308	5.4086	10.6249	8.3489
	313	5.5752	12.5981	9.6035
	318	5.7093	14.1160	10.5080

from the surface of the solid into the bulk of liquid [24].

As shown in Table 1, the effective diffusion coefficient and mass transfer coefficient for the ultrasound-assisted extraction of paclitaxel from *Taxus chinensis* were calculated by plotting $\ln (Y_s/(Y_s-Y_t))$ versus t and $\ln (C_s/(C_s-C_t))$ versus t, respectively. The effective diffusion coefficient, mass transfer coefficient, and Biot number, according to the ultrasound power and extraction temperature, are presented in Table 3. The effective diffusion coefficients increased with increasing temperature and ultrasound power. The obtained value of D_e ($4.1882 \times 10^{-13} \sim 5.7093 \times 10^{-13}$ m^2/s) is much lower than that for the extraction of alkaloids from *Atropa belladonna* with methanol ($2.52 \times 10^{-10} \sim 4.79 \times 10^{-10}$ m^2/s), and for the extraction of lignans flaxseed meal with water ($2 \times 10^{-13} \sim 9 \times 10^{-13}$ m^2/s), and much higher than that for the extraction of andrographolide from *Andrographis paniculate* with water (6.67×10^{-14} m^2/s) [24]. The mass transfer coefficients ($4.7053 \times 10^{-8} \sim 14.1160 \times 10^{-8}$ m/s) increased on a proportionally much larger scale than the effective diffusion coefficient. While the increase in the diffusion coefficient may be attributed to increased thermal energy at higher temperatures and ultrasound powers, the increase in the mass transfer coefficient could be attributed to both an increase in the diffusion coefficient and a decrease in viscosity [22,30]. This would likely explain the higher influence of temperature and ultrasound power on the mass transfer coefficient than that on the diffusion coefficient. Therefore, the mass transfer Biot number (4.8-10.5) increased with temperature and ultrasound power. The higher values of Biot number indicates that the external resistances for mass transfer is negligible, confirming efficient mixing between solute and solvent, and therefore, internal transfer is rate-limiting [22]. These results are similar to those observed in the extraction of phenol from the oak chips of wines [31,32].

4. Conclusions

In this study, ultrasound-assisted extraction was performed for the efficient recovery of paclitaxel from *Taxus chinensis*, with the kinetics and mechanism of extraction process being analyzed. Most of the paclitaxel (~99%) was recovered from biomass by a single extraction under an optimum ultrasound power of 380 W and extraction time of 10 min. The number of cavitation bubbles increased with increasing ultrasound power, which promoted cell disruption, and consequently the extraction process, due to the collapse of these bubbles. The extraction kinetics was described very well by the pseudo-second-order kinetic model, while intraparticle diffusion played a dominant role in pacltaxel extraction from biomass in accordance with the intraparticle diffusion model. The effective diffusion coefficient (4.1882×10^{-13}-5.7093×10^{-13} m^2/s), mass transfer coefficient (4.705×10^{-8}-14.1160×10^{-8} m/s), and Biot number (4.8-10.5) increased with increasing temperature and ultrasound power, indicating that the external resistances for mass transfer are negligible, confirming efficient mixing between solute and solvent and therefore, internal transfer is rate-limiting.

Acknowledgement

This work was supported by the research grant of the Kongju National University in 2018.

References

1. Kim, J. H. (2006) Paclitaxel: recovery and purification in commercialization step. *Korean J. Biotechnol. Bioeng*. 21: 1-10.
2. Bang, S. Y. and J. H. Kim (2017) Isotherm, kinetic, and thermodynamic studies on the adsorption behavior of 10-deacetylpaclitaxel onto Sylopute. *Biotechnol. Bioproc. Eng*. 22: 620-630.
3. Kim, G. J. and J. H. Kim (2015) Enhancement of extraction efficiency of paclitaxel from biomass using ionic liquid-methanol co-solvents under acidic conditions. *Process Biochem*. 50: 989-996.
4. Kim, H. S. and J. H. Kim (2017) Kinetics and thermodynamics of microwave-assisted drying of paclitaxel for removal of residual methylene chloride. *Process Biochem*. 56: 163-170.
5. Rao, K. V., J. B. Hanuman, C. Alvarez, M. Stoy, J. Juchum, R.M. Davies, and R. Baxley (1995) A new large-scale process for taxol

and related taxanes from *Taxus brevifolia*. *Pharm. Res*. 12: 1003-1010.
6. Baloglu, E. and D. G. I. Kingston (1999) A new semisynthesis of paclitaxel from baccatin III. *J. Nat. Prod*. 62: 1068-1071.
7. Choi, H. K., S. J. Son, G. H. Na, S. S. Hong, Y. S. Park, and J. Y. Song (2002) Mass production of paclitaxel by plant cell culture. *Korean J. Plant Biotechnol*. 29: 59-62.
8. Shin, H. S. and J. H. Kim (2016) Isotherm, kinetic and thermodynamic characteristics of adsorption of paclitaxel onto Diaion HP-20. *Process Biochem*. 51: 917-924.
9. Kim, J. H. (2000) Optimization of extraction process for mass production of paclitaxel from plant cell cultures. *Korean J. Biotechnol. Bioeng*. 15: 346-351.
10. Živković, J., K. Šavikin, T. Janković, N. Ćujić, and N. Menković (2018) Optimization of ultrasound-assisted extraction of polyphenolic compounds from pomegranate peel using response surface methodology. *Sep. Purif. Technol*. 194: 40-47.
11. Cheung, Y. C. and J. Y. Wu (2013) Kinetic models and process parameters for ultrasound-assisted extraction of water-soluble components and polysaccharides from a medicinal fungus. *Biochem. Eng. J*. 79: 214-220.
12. Alessandro, L. G., K. Kriaa, I. Nikov, and K. Dimitrov (2012) Ultrasound assisted extraction of polyphenols from black chokeberry. *Sep. Purif. Technol*. 93: 42-47.
13. Zhongli, P., Q. Wenjuan, M. Haile, G. A. Griffiths, and H. M. Tara (2011) Continuous and pulsed ultrasound-assisted extractions of antioxidants from pomegranate peel. *Ultrason. Sonochem*. 18: 1249-1257.
14. Ramandi, N. F., A. Ghsssempour, N. M. Najafi, and E. Ghasemi (2017) Optimization of ultrasonic assisted extraction of fatty acids from *Borago officinalis* L. flower by central composite design. *Arabian J. Chem*. 10: S23-S27.
15. Lee, C. G. and J. H. Kim (2017) A kinetic and thermodynamic study of fractional precipitation of paclitaxel from *Taxus chinensis*. *Process Biochem*. 59: 216-222.
16. Kim, T. W. and J. H. Kim (2016) Kinetics and thermodynamics of paclitaxel extraction from plant cell culture. *Korean J. Chem. Eng*. 33: 3175-3183.
17. Ha, G. S. and J. H. Kim (2016) Kinetic and thermodynamic characteristics of ultrasound-assisted extraction for recovery of paclitaxel from biomass. *Process Biochem*. 51: 1664-1673.
18. Langergren, S. and B. K. Svenska (1898) Zur theoie der sogenannten adsorption geloester stoffe. *Veter. Hand*. 24: 1-39.
19. Rakotondramasy-Rabesiaka, L., J. L. Havet, C. Porte, and H. Fauduet (2007) Solid-liquid extraction protopine from *Fumaria officinalis* L.-Analysis determination, kinetic reaction and model building. *Sep. Purif. Technol*. 54: 253-261.
20. Ho, Y. S., H. A. Harouna-Oumarou, H. Fauduet, and C. Porte (2005) Kinetics and model building of leaching of water-soluble compounds of *Tilia* sapwood. *Sep. Purif. Technol*. 45: 169-173.
21. Weber, W. J. and J. C. Morris (1963) Kinetics of adsorption on carbon from solution. *J. Sanit. Eng. Div. Am. Soc. Civ. Eng*. 89: 31-59.
22. Krishnan, R. Y. and K. S. Rajan (2016) Microwave assisted extraction of flavonoids from *Terminalia bellerica*: Study of kinetics and thermodynamics. *Sep. Purif. Technol*. 157: 169-178.
23. Krishnan, R. Y., M. N. Chandran, V. Vadivel, and K. S. Rajan (2016) Insights on the influence of microwave irradiation on the extraction of flavonoids from *Terminalia chebula*. *Sep. Purif. Technol*. 170: 224-233.
24. Rakotondramasy-Rabesiaka, L., J. L. Havet, C. Porte, and H. Fauduet (2010) Estimation of effective diffusion and transfer rate during the protopine extraction process from *Fumaria officinalis* L. *Sep. Purif. Technol*. 76: 126-131.
25. Davoud, S., S. F. B. Bibi, M. K. Mohamad, S. N. Zahra, K. Farhad, and S. Amirhossein (2014) Oil stability index and biological activities of *Achillea biebersteinii* and *Achillea wilhelmsii* extracts as influenced by various ultrasound intensities. *Ind. Crop. Prod*. 55: 163-172.
26. John, F. (2011) Ultrasonics - number and size of cavitation bubbles, Cleaning Technologies Group, Available from: http://techblog.ctgclean.com/2011/12/ultrsonics-number-and-size-of-cavitation-bubbles.
27. Meziane, S. and H. Kadi (2008) Kinetics and thermodynamics of oil extraction from olive cake. *J. Am. Oil Chem. Soc*. 85: 391-396.
28. Qu, W., Z. Pan, and H. Ma (2010) Extraction modeling and activities of antioxidants from pomegranate mare. *J. Food. Eng*. 99: 16-23.
29. Kavitha, D. and C. Namasivayam (2007) Experimental and kinetic studies on methylene blue adsorption by coir pith carbon. *Bioresour. Technol*. 98: 14-21.
30. Ji, J., X. Lu, M. Cai, and Z. Xu (2006) Improvement of leaching process of geniposide with ultrasound. *Ultrason. Sonochem*. 13: 455-462.
31. Skerget, M. and Z. Knez (2001) Modelling high pressure extraction processes. *Comput. Chem. Eng*. 25: 879-886.
32. Tao, Y., Z. Zhang, and D. Sun (2014) Experimental and modeling studies of ultrasound-assisted release of phenolics from oak chips into model wine. *Ultrason. Sonochem*. 21: 1839-1848.